CORRELATION BETWEEN MORPHOLOGICAL, OPTICAL AND ELECTRICAL PROPERTIES OF ZnO:AL/ZnO DOUBLE LAYERS AND THE $Cu(In,Ga)Se_2$ SOLAR CELL EFFICIENCIES

PD Nsimama
Department of Science and Laboratory Technology, Dar Es Salaam Institute of Technology,
P.O. Box 2958, Dar Es Salaam-Tanzania.
E-mail: pnsimama@yahoo.com, Nsimama@dit.ac.tz

ABSTRACT

The morphological, optical and electrical properties of magnetron sputtered ZnO:Al/ZnO double layers are reported and their correlations with their respective $Cu(In,Ga)Se_2$ (CIGS) solar cell efficiencies are presented. The ZnO:Al/ZnO double layers were produced by using the established baseline RF process and plasma emission monitoring (PEM) DC reactive sputtering. The scanning electron microscope (SEM) and atomic force microscope (AFM) were employed for the surface morphological measurements. The charge carrier concentrations, mobilities and AC resistivities were deduced from Drude's model. The DC resistivities were determined from the four-point probe measurements. Transmittance and reflectance measurements were done by using the UV-VIS-NIR Lambda 900 double beam spectrophotometer. The I-V characteristic technique was employed for the solar cell performances. The lowest AC and DC resistivities obtained were 3.69 and 10.37ohm.cm respectively. Transmittances approaching 90% have been recorded by the ZnO:Al/ZnO double layers. Lower CIGS solar cell efficiencies were those fabricated from ZnO:Al/ZnO double layers with non-uniform AFM surfaces.

Keywords: ZnO:Al/ZnO, $Cu(In,Ga)Se_2$, sputtering, efficiency, Drude model.

INTRODUCTION

CIGS thin film solar cells seem to be the promising candidates for future clean energy after reaching the efficiency approaching 20% (Contreras *et al.* 1999). Several measures have taken place in a couple of years to take CIGS solar cells to that landmark, including the introduction of a wide bandgap material Ga into $CuInSe_2$ to form $Cu(In,Ga)Se_2$ and the use of soda lime glass substrate instead of a hard glass substrate; both of which have lead to the increase in Voc (Kronik *et al.* 1998). Another positive development was recorded when the chemical bath deposition CdS buffer layer replaced that which was produced by the physical vapour deposition technique (Herrero *et al.* 2000, Ramadhani *et al.* 1998). The role of the CBD-CdS is to facilitate the diffusion of Cd into the CIGS absorber and the formation of the buried p-n junction inside the absorber. It also serves as a protection of the junction region from sputtering damage during subsequent transparent conducting oxide (TCO) depositions (Hamakawa 2004).

Another improvement in the cell performance was reported (Lee *et al.* 2000) to be obtained when ZnO:Al/ZnO double layer window was employed to replace the undoped ZnO single layer. Sputter deposition of a ZnO film has been known to damage the underlying layer and produce defects and dislocations at the interface. This is due to the collisions of high energetic particles released from the target. In order to prevent the disadvantages of sputtering in fabricating solar cells, bi-layer ZnO films are employed to improve the cell performance (Lee *et al.* 2000). The study of how different morphological, optical and

electrical properties influence the performances of CIGS solar cells will pave a way for the improvement of the future CIGS solar cells. Ishizuka and his co-workers (2005) studied the correlation of ZnO/ZnO:Al double layers on the CIGS solar cells performance by varying the thickness of ZnO. They reported a ZnO/ZnO:Al thickness of 70 nm as the optimum one for the best performance CIGS solar cell.

There is little work in the literature reporting on the correlation of the properties of the TCO double layers with the CIGS solar cell performances. In the current work, a detailed account on the correlation of ZnO:Al/ZnO double layer properties with their respective CIGS solar cell efficiencies is given. The ZnO:Al/ZnO double layers were deposited by changing the deposition parameters of ZnO:Al films while fixing those of the ZnO.

EXPERIMENTAL DETAILS

The established baseline process (Kessler *et al.* 2001) was employed for fabricating the CdS/CIGS/Mo/SLG stack. The detailed CIGS solar cell fabrication process and the optimizations of ZnO and ZnO:Al layers can be found elsewhere (Nsimama *et al.* 2008). Thereafter, a double layer ZnO/ZnO:Al was deposited to finish the fabrication process. The coating system used in depositing ZnO and ZnO:Al films was from VON ARDENNE ENLARGENTECHNIK GMBH. The chamber was evacuated to an ultimate pressure of 1 x 10^{-7} Torr, before introducing the argon gas (purity 99.9997%) through the mass flow controller. The deposition of ZnO and ZnO:Al was done in two stages; First by using the baseline process where the ZnO/ZnO:Al (respectively, 100 and 400nm) was sputtered by radio frequency (RF) process from ZnO:Al ceramic targets (purity 99.9999%) with radius 5 cm. Secondly, the RF ZnO/DC ZnO:Al double layer was deposited with ZnO:Al being prepared from the Zn:Al (Zn 98% + Al 2%) target (purity 99.999%) with radius 5 cm metallic target at different deposition parameters. The oxygen gas (purity 99.998%) was thereafter introduced into the chamber via a plasma emission monitoring (PEM) control system which was controlling the amount of oxygen in the chamber.

The deposition conditions for the ZnO:Al films used in preparing ZnO:Al/ZnO double layers (the baseline process and three DC reactively sputtered) are as shown in Table 1. In all the cases, the ZnO was deposited using the baseline RF process. For DC1, DC2 and DC3, the changes in ZnO/ZnO:Al double layers were brought by different deposition conditions of ZnO:Al layers.

Table 1: Deposition conditions for the ZnO/ZnO:Al double layers for different $Cu(In,Ga)Se_2$ solar cells.

Cell /ZnO:Al	Deposition rate (nm/min)	Argon flow rate (ml/min)	PEM setpoint (%)	Power (W)
RF (Baseline)	115.2	10	-	300
DC 1	61.8	10	42	100
DC 2	135.2	50	44	200
DC 3	134.4	50	48	200

The sheet resistance measurements were done by using a Veeco FPP 5000 four-point probe. Thickness measurements were done by using a Dektak 2000 Si surface

profilometer after producing a step by etching. SEM pictures were taken by Philips Lybold 20. The AFM images were taken by a Digital Instruments Nanoscope IIIa Multimode atomic force microscope in a taping mode. The transmittance (T) and reflectance (R), measurements were carried out at room temperature with unpolarized light at normal incidence in the wavelength range 300 – 2500 nm, with a double-beam spectrophotometer (Perkin Elmer Lambda 900) equipped with an integrating sphere coated with $BaSO_4$.

The charge carrier concentration and mobility of the films were determined from the Drude model. The exercise involved four stages, namely; Defining the optical constants in which the high frequency permeability, $\varepsilon_\infty = 3.85$ was used, since the literature (Jin *et al*. 1988) shows that $\varepsilon_\infty = 3.85 \pm 0.1$ irrespective of the doping, defining layer stacks, simulating spectra and fitting the parameters. The layer stack was vacuum/ZnO/ZnO:Al/glass/vacuum and the simulated spectra were the transmittance(T) and reflectance (R). The fitting parameters employed were the damping constant (γ), plasma frequency (ω_p) and film thickness (t). The optical bandgap was calculated from Tauc relation through extrapolation of the plot of $(\alpha h\upsilon)^2$ against $h\upsilon$.

RESULTS AND DISCUSSION

Morphological properties

SEM results

Figure 1 shows the SEM images for the ZnO:Al/ZnO double layers for the baseline (RF), DC1, DC2 and DC3 CIGS solar cells. The surfaces of ZnO:Al/ZnO double layers for RF, DC1 and DC3 solar cells are having some finger-like horizontal shapes with that of DC1 showing some better defined grains. Few vertical finger-like shapes are also observed. For the ZnO:Al/ZnO double layer of DC2 CIGS solar cell, the SEM image has no vertical-like shapes observed in the rest of the cells. However, there isn't any significant difference among the images.

AFM results

The AFM images for the ZnO/ZnO:Al double layers used in fabricating different CIGS solar cells are shown in Figure 2. The AFM images are displayed in three profiles namely; 3D-height, 2D-height and 3D-phase. It is clear from the images that the ZnO:Al/ZnO double layer used in fabricating the RF (Figure 2 (a)) and DC1 (Figure 2 (b)) CIGS solar cells have uniformly distributed grain particles. However, the ZnO:Al/ZnO double layers used in fabricating DC2 and DC3 solar cells have non-uniform surfaces as can be observed in the 3D-height profiles. The intensity of the colour reflects the height of the particles. The 2D-height distribution of the ZnO:Al/ZnO double layers for cells DC2 and DC3 solar cells show a high level of non-uniformity in heights of the deposited particles as can be substantiated by the mixture of black, red, orange and white colours on the films.

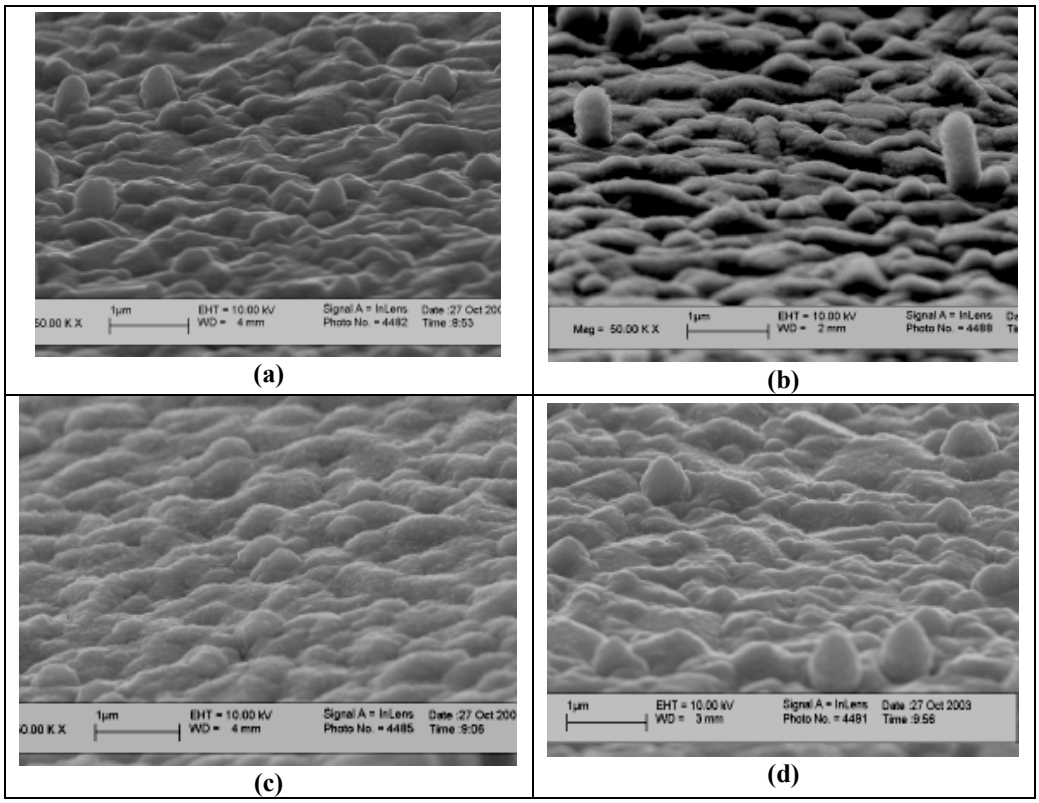

Figure 1: SEM plain view images for ZnO:Al/ZnO double layers used to fabricate (a) Baseline (RF) solar cell (b) DC1 solar cell (c) DC2 solar cell and (d) DC3 CIGS solar cell.

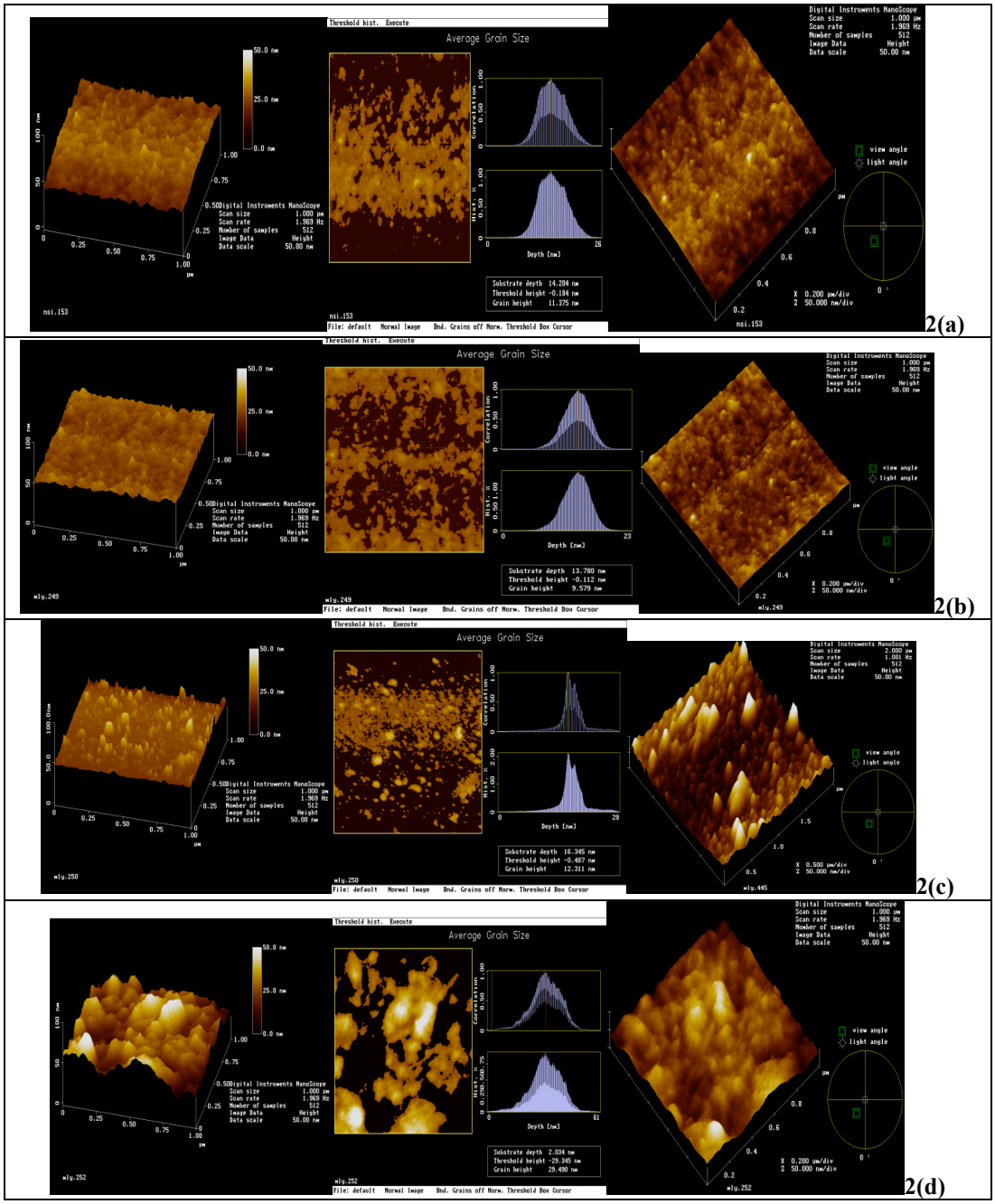

Figure 2 The AFM images in 3D-height, 2D-height and 3D-phase profile for ZnO/ZnO:Al double layers used to fabricate CIGS solar cells; (a) Baseline (RF) (b) DC1 (c) DC2 and (d) DC3.

The average particle height for the ZnO:Al/ZnO double layers used in fabricating RF, DC1, DC2 and DC3 were 11.38 nm, 9.58 nm, 12.31 nm and 29.45 nm respectively. The large grain size of the last double layer is possibly due to the uneven distribution of the particles as revealed by Figure 2(d), where grains heaped on few positions. The ZnO:Al/ZnO double layer for DC1 solar cell has the best distribution of particles in the 2D-height profile.

Optical properties

Transmittance

Figure 3 shows the transmittance of ZnO:Al/ZnO double layers for the RF, DC1, DC2 and DC3 CIGS solar cells. It can be observed from the results that all the films are highly transmitting in the near-infrared and visible regions with transmittance greater than 78%. The ZnO:Al/ZnO double layer for cell DC1 shows superior transmission in the mentioned region, with its transmittance being above 80%. The average transmittance results for the ZnO:Al/ZnO layers shown by the in-set figure substantiates its transmission superiority. The reason for this is possibly due to its smallest thickness of the rest double layers and a good film uniformity as observed in AFM images in Figure 2(b). All the films have a sharp absorption edge in the UV range of 300-400nm. The transmittance decreased in the near-infrared region, which mainly came from the increase of reflectance due to the plasma resonance of electron gas in the conduction band (Gong *et al*. 2010).

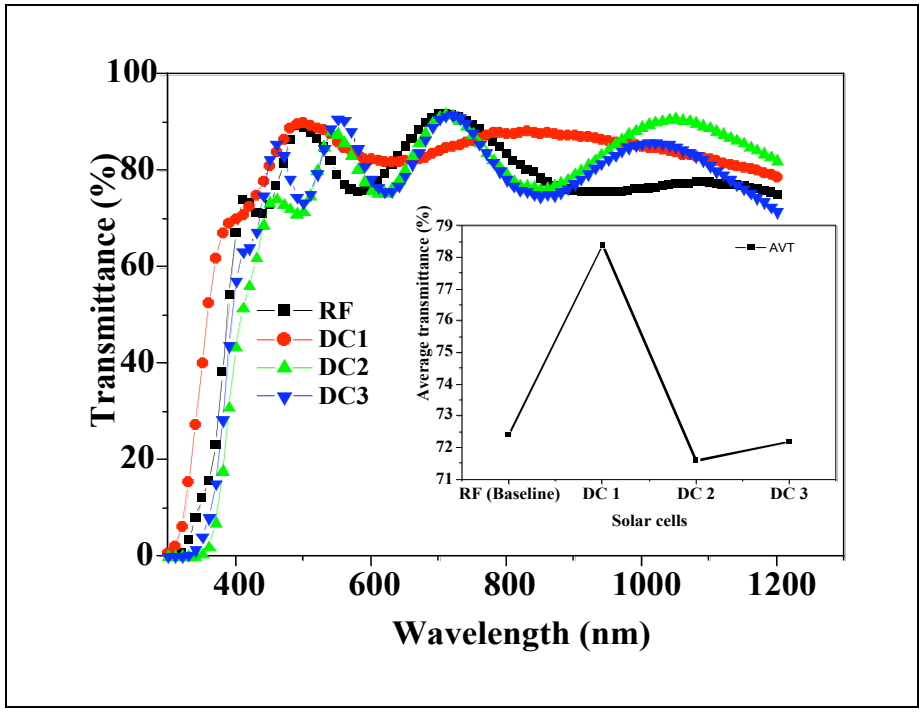

Figure 3 The transmittance of ZnO:Al/ZnO double layers for RF, DC 1, DC 2 and DC 3 CIGS solar cells

Optical bandgap

The optical bandgap for the ZnO:Al/ZnO layers of different CIGS solar cells varied as shown in Figure 4. The general formula for determining the optical bandgaps is given (Harding *et al*. 1991) by

$$(\alpha h\upsilon)^{1/n} = B(h\upsilon - E_{opt}) \qquad (1),$$

where B is a constant and n depends on the type of transition. For the indirect allowed, direct forbidden and direct allowed transition the values of n are 2, $\frac{3}{2}$ and $\frac{1}{2}$ respectively.

ZnO involves a direct allowed transition and its corresponding relation (Harding *et al* 1991) is

$$(\alpha h\upsilon)^2 = B(h\upsilon - E_{opt}) \qquad (2)$$

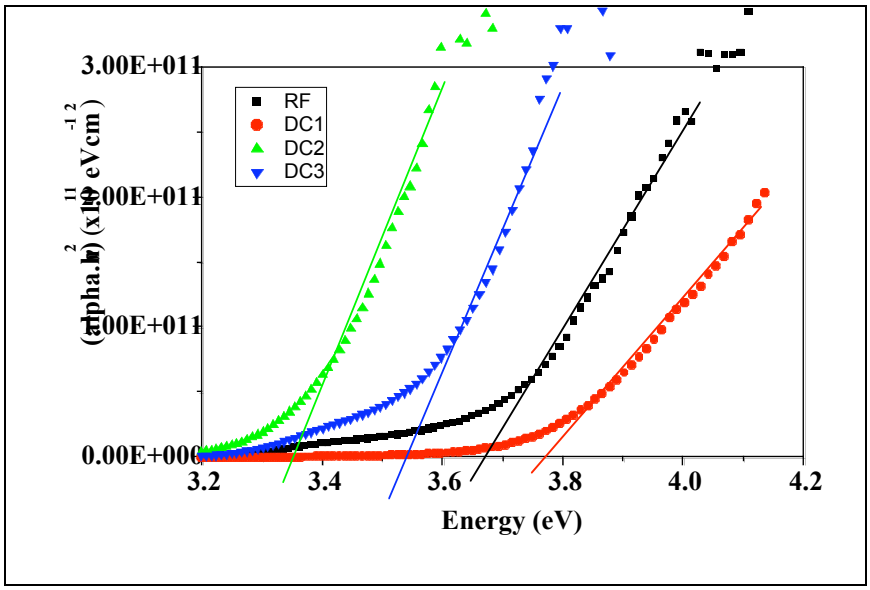

Figure 4; The plot of $(\alpha h\upsilon)^2$ with energy hυ for the determination of optical bandgaps of ZnO:Al/ZnO double layers for RF, DC 1, DC2 and DC3 CIGS solar cells.

The optical bandgaps are obtained by extrapolating the plot of $(\alpha h\upsilon)^2$ against the energy (hυ).
The x- intercept on the x- axis ($\alpha = 0$), gives E_{opt}, the optical bandgap.

The absorption coefficient of the films is calculated using the equation (Harding *et al*. 1991)

$$\alpha = \frac{1}{d}\ln\left[\frac{(1-R)^2}{2T} + \left\{\frac{(1-R)^4}{4T^2} - R^2\right\}^{0.5}\right] \qquad (3)$$

Where d stands for the thickness, R is the reflectance and T is the transmittance.

The bandgaps of the ZnO:Al/ZnO double layers used in fabricating solar cells DC2, DC3, RF and DC1 were 3.35, 3.54, 3.67 and 3.77eV respectively. This trend is in agreement with the transmittance results shown in Figure 3, in which the transmittance data showed an increasing trend for the double layers of the respective cells.

Electrical properties

The Drude parameters are involved in the classical oscillator model for free charge carriers where the real part $\varepsilon_1(\omega)$ of the dielectric function can be written (Brehme *et al*. 1999) as

$$\varepsilon_1(\omega) = \varepsilon_\infty - \frac{\omega_p^2}{\omega^2 + \gamma^2} \qquad (4)$$

Where, ε_∞, is the high-frequency dielectric constant including the interband contribution, γ, the damping constant and ω_p, is the plasma frequency.

The damping constant, γ is related to the mobility, μ by the relation (Sing *et al* 2001)

$$\gamma = \frac{e}{\mu m_e^*} \qquad (5)$$

And the plasma frequency, ω_p is related to the charge carrier concentration, N by the relation (Brehme *et al*. 1999)

$$\omega_p^2 = \frac{Ne^2}{\varepsilon_0 \varepsilon_\infty m_e^*} \qquad (6)$$

where N is the charge carrier concentration, e is the electron charge, m_e^* is the effective mass of electron in the conduction band and ε_0 is the permittivity of free space. $m_e^* = 0.28\ m_e$, where m_e is the free electron mass.

The AC resistivity, ρ_{AC} is determined from the relation (Hong *et al* 2003)

$$\rho_{AC} = \frac{\gamma m^*}{N_e^2} = \frac{1}{\mu N e} \qquad (7)$$

Figure 5 (a) shows the variation of CIGS solar cell efficiencies with the ZnO:Al/ZnO double layers resistivities. There is an inversely proportional relationship between the solar cell efficiencies and their respective ZnO:Al/ZnO double layer resistivities as expected. The highest efficiency CIGS solar cell, i.e., DC1 comes from ZnO:Al/ZnO double layer with the lowest resistivity. The lowest resistivity is attributed to its smallest thickness (Table 1), and the surface film uniformity as revealed in the AFM images (Figure 2 (b)).

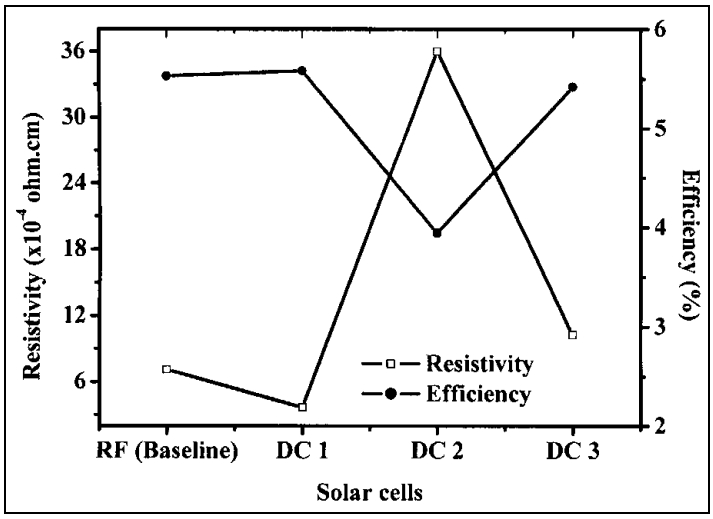

Figure 5 (a) The variation of CIGS solar cell efficiencies with their respective ZnO:Al/ZnO double layer resistivities.

Generally, all cells have comparable efficiencies with the exceptional of the DC2 solar cell, whose efficiency is less than 20%. This low efficiency is possibly due to the high argon flow rate (50ml/min) used in the film preparation, since at high argon flow rate there is a deterioration of grains due to electron bombardment in the plasma to the substrate (Fu *et al*. 2004). The non-uniform 2D-height particle distribution AFM image of DC2 double layer from Figure 2(c) explains the low efficiency. The PEM setpoint is possibly what brings the difference between the properties of DC2 and DC3 double layers, since it is the only deposition parameter separating the two; the rest of the deposition parameters were the same.

To confirm the utility of the Drude optical approximation of the electrical properties, the variation of the DC resistivity from the Four-point probe for all ZnO:Al/ZnO double layers used in fabricating CIGS solar cells was carried out. The result is shown by Figure 5(b). The trend for both techniques is the same with Drude resistivity values being lower than those obtained from the Four-point probe (DC resistivity). The Drude values are obtained by sampling the carrier motion at optical frequencies where the monitored transport paths are smaller than the grain size and thus the probability of crossing a grain boundary is low (Brehme *et al.*1999). Therefore, its resistivity values are supposed to be significantly lower than those coming from the direct measurements, which concur with the results from the current work. It can also be noted that DC ZnO:Al films deposited at the PEM setpoints higher than 42% gave relatively higher resistivities. This suggests that 42% PEM setpoint is the optimum point for the resistivity.

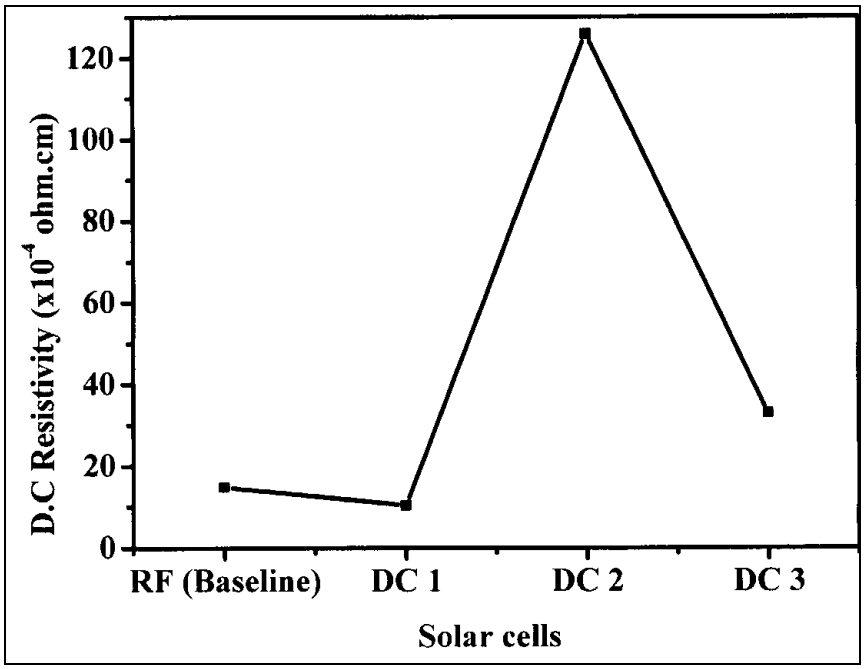

Figure 5 (b) The variation of CIGS solar cell efficiencies with their respective ZnO:Al/ZnO resistivities.

The variation of charge carrier concentration and mobility for CIGS solar cells fabricated using different ZnO:Al/ZnO double layers is shown in Figure 6. It is clear from the results that the trend of charge carrier concentration and mobility for the DC reactively sputtered ZnO:Al/ZnO double layers is similar, suggesting that both parameters are core for the determination of efficiencies in CIGS solar cells. The lowest resistivity recorded by the ZnO:Al/ZnO double layer of the DC1 solar cell is possibly due to the higher values of both carrier concentration and mobility which tends to decrease the resistivity (Kon *et al*. 2002).

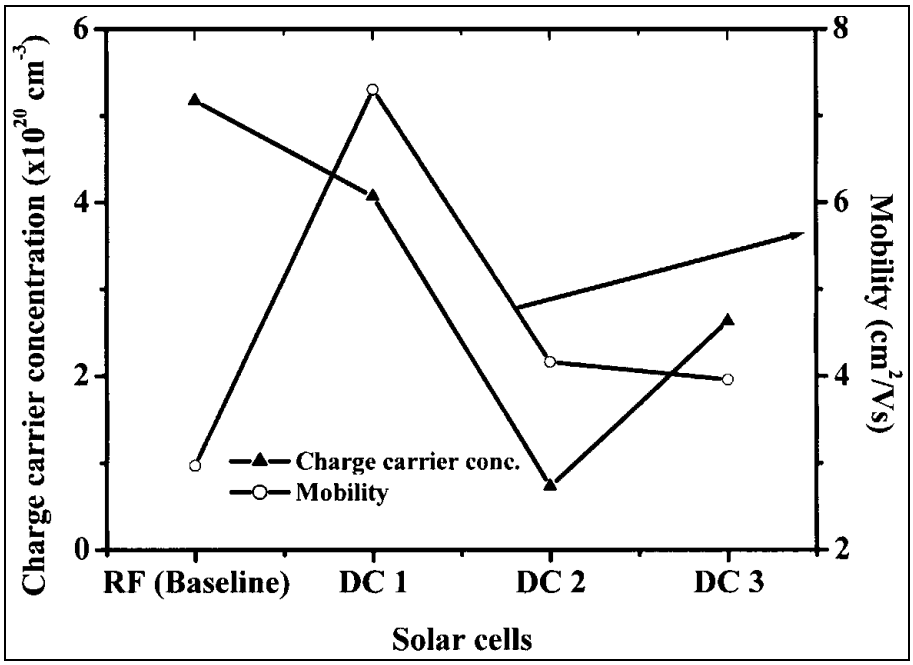

Figure 6 The variation of ZnO:Al/ZnO charge carrier concentration and mobility with the solar cell efficiency.

The low mobility of the ZnO:Al/ZnO double layer is possibly due to the higher value of power (300W) which tends to increase the defects in the film due to fast growth rate and bombardment of energetic ion and neutral species during the deposition (Malinovska *et al*. 1998). It is worth noting that the low mobility of the ZnO:Al/ZnO double layer for the RF CIGS solar cell didn't affect much of its efficiency as can be observed in Figure 5(a). This suggests that the carrier concentration is the sole factor for the efficiency of CIGS solar cells fabricated using the RF technique. The detailed performance analysis of the solar cells in the current work, including all important parameters such as open circuit voltage (Voc) short circuit current density (Jsc), Fill Factor (FF) and quantum efficiency (QE) can be found elsewhere (Nsimama *et al*. 2008). It was reported that DC 1 CIGS solar cell gave the highest FF, QE Jsc and efficiency values.

CONCLUSION

The ZnO:Al/ZnO double layers have successfully been prepared using RF and DC sputtering and the correlation of their morphological, optical and electrical properties with their respective CIGS solar cell performances has been established. There is a strong correlation between the properties of the ZnO:Al/ZnO double layers with CIGS solar cell efficiencies. The ZnO:Al/ZnO double layers with uniform AFM image surfaces, high transmittance, optical bandgap and low resistivity correlated with higher CIGS solar cell efficiencies. For CIGS solar cells fabricated using the DC reactive sputtering process, their efficiencies vary proportionally with the charge carrier concentration and the mobility. DC ZnO:Al/ZnO double layers deposited at higher argon flow rates and DC powers recorded relatively lower solar cell efficiencies.

ACKNOWLEDGEMENTS

This work was sponsored by the International Science Program (ISP), Uppsala-Sweden. The assistance in AFM measurements from Dr. N. Mlyuka of the Department of Physics, University of Dar Es Salaam, Tanzania is highly acknowledged.

REFERENCES

Brehme S, Fenske F, Fuhs W, Nebauer E, Poschenrieder M, Selle B, Sieber I 1999 Free-carrier plasma resonance effects and electron transport in reactively sputtered degenerate ZnO:Al films. *Thin Solid Films* **342**:167-173.

Contreras MA, Egaas B, Ramanathan K, Hiltner J, Swartzlander A, Hasoon F, Noufi R 1999 Efforts toward 20% efficiency in $Cu(In,Ga)Se_2$ polycrystalline thin-film solar cells. *Prog. Photovolt: Res. Appl.* **7**: 311-316.

Fu EG, Zhuang DM, Zhang G, Ming Z, Yang WF, Liu JH 2004 Properties of transparent conductive ZnO:Al thin films prepared by magnetron sputtering. *Microelectron. J.* **35**:383-316.

Gong L, Ye Z, Lu J, Zhu L, Huang J, Gu X, Zhao B, 2010 Highly transparent conductive and near-infrared reflective ZnO:Al thin films. *Vacuum* **84**:947-947.

Hamakawa Y 2004 Next generation photovoltaic and its applications. Verlag Berlin Heidelberg: Springer.

Harding GL, Window B, Horrigan EC 1991Studies on ZnO:Al thin films deposited by in-line reactive mid-frequency magnetron sputtering. *Sol. Energy Mater. Sol. Cells* **22**:69-91.

Herrero J, Gutiérrez MT, Guillén C, Doña JM, Martinez MA, Chaparro AM, Bayón R 2000 Photovoltaic windows by chemical bath deposition. *Thin solid films* **361-362**:28-33.

Hong RJ, Jiang X, Szyszka B, Sittinger V, Pflug A, 2003 Studies on ZnO:Al thin films deposited by in-line reactive mid-frequency magnetron sputtering. *Appl. Surf. Sci.* **207**:341-350.

Ishizuka S, Sakurai K, Yamada A, Matsubara K, Fons P, Iwata K, Nakamura S, Kimura Y, Baba T, Nakanishi H, Kojima T, Niki S 2005 Fabrication of wide-gap $Cu(In_{1-x}Ga_x)Se_2$ thin films solar cells: a study on the correlation of cell performance with highly resistive i-ZnO layer thickness. *Sol. Energy Mater. Sol. Cells* **87**:541-548.

Jin ZC, Hamberg I, Granqvist CG, 1988 Optical properties of sputter-deposited ZnO:Al thin films. *J. Appl. Phys*. **64**:5117-5131.

Ramanathan K, Wiesner H, Asher S, Niles D, Bhattacharya RN, Contreras MA and Noufi R 1998 High-efficiency $Cu(In,Ga)Se_2$ thin film solar cells without intermediate buffer layers. *NREL/CP*-520-23898.

Kessler J, Bodegärd M, Hedström J and Stolt L 2001 Baseline $Cu(In,Ga)Se_2$ device production: control and statistical significance. *Sol. Energy Mater. Sol. Cells* **67**:67-76.

Kon M, Song PK, Mitsui A and Shigesato Y 2002 Crystallinity of Gallium-doped zinc oxide films deposited by DC magnetron sputtering using Ar, Ne or Kr gas. *Jpn. J. Appl. Phys*. **41**: 6174-6179.

Kronik L, Cahen D and Chock HW 1998 Effects of sodium on polycrystalline $Cu(In,Ga)Se_2$ and its solar cell performance. *Adv. Mater.* **10**:31-36.

Lee JC, Kang KH, Kim SK, Yoon KH, Park IJ and Song J 2000 RF sputter deposition of the high-quality intrinsic and n-type ZnO window layers for $Cu(In,Ga)Se_2$-based solar cell applications. *Sol. Energy Mater. Sol. Cells* **64**:185-195.

Malinovska DD, Tzenov N, Tzolov M and Vassilev L 1998 Optical and electrical properties of R.F. Magnetron sputtered ZnO:Al thin films. *Mater. Sci. Eng. B* **52**:59-62.

Nsimama PD, Samiji ME, Mbise GW and Niklasson GA, Wennerberg J. Edoff M 2008 Performance comparison of Cu(In,Ga)Se_2 solar cells fabricated using RF and DC sputtered ZnO:Al transparent conducting oxides. *Phys. Status Solid C* **5**:612-615.

Singh AV, Kumar M, Mehar RM, Wakahar A and Yoshida A 2001 Al-doped zinc (ZnO:Al) thin films by pulsed laser ablation. *J. India Inst. Sci.* **81**:527-532.

Wang WW, Diao XG, Wang Z, Yang M, Wang TM and Wu Z 2005 Preparation and characterization of high-performance direct current magnetron sputtered ZnO:Al. *Thin Solid Films* **491**:54-60.